Evaluation of initialization procedures for estimating upper limb kinematics with MARG sensors

Daniel Galinski and Bruno Dehez, *Member, IEEE*

***Abstract*—Instrumentation able to estimate upper limbs kinematics has a lot of relevance in the context of rehabilitation of stroke patients. The systems based on inertial systems seem to be well suited for clinical environment and numerous authors have presented wearable systems interesting in terms of accuracy and easiness of implementation. These systems always require an initialization procedure and the authors do not justify clearly why they are using one method rather than another. In this paper two common initialization methods are presented and they are evaluated and compared on the basis of the kinematics tracking of upper limbs daily living activities. The experimental results show that an initialization based on functional axes is less sensitive to the respect of initialization conditions than a static initialization.**

***Index Terms*—Joint angle measurement, upper limb, MARG, MIMU, IMMS, Inertial measurement, initialization procedure.**

I. Introduction

STROKE that results in partial or complete hemiparesis is the main cause of disability [1]. One of the goals of stroke rehabilitation is to regain the highest level of motor function in order to recover the highest independence daily living activities (using lower and upper limbs). In this rehabilitation context, instrumentation able to measure limb kinematics has mainly two uses. On the one hand, such a device permits to obtain a quantitative evaluation of rehabilitation and pharmacological treatment effects by measuring residual motor skills. It also allows to provide a quantified evaluation of the progress of the patient [2]. On the other hand, such a device may serve as an input for a virtual visual feedback which has demonstrated benefits in motor recovery for patients after a stroke [3]–[5]. This paper is mainly concerned with the upper limb kinematics estimation.

Many solutions exist and can be classified in three categories [6]: i) Visual tracking (marker or marker-free based); ii) Robot-aided tracking or; iii) Non-visual tracking (inertial, magnetic and others). The fact that these kinematics measurements are done in a clinical environment during revalidation sessions imposes lots of constraints. The device must be lightweight and wearable. In addition, it must not require dedicated room and long calibration and installation time. Considering these requirements and the survey established by Zhou et al. [6], inertial systems seem to be the most suited for an utilization during rehabilitation sessions.

Inertial solutions can be named as magnetic, angular rate and gravity sensors (MARG) if they are composed of gyroscopes, accelerometers and magnetometers. Current solutions use effective fusion algorithms in order to obtain from these sensors the absolute orientation in the Earth frame without drift [7]. In recent years, many systems have been developed for the ambulatory measurement of segment motion, e.g. Picerno et al. [8], van Acht et al. [9] or Luinge et al. [10].

As the sensors can not be placed on the limb with a well known orientation, an initialization procedure is mandatory in order to find their relative orientation to the skeleton. Four main initialization approaches emerge from the literature: measuring the gravity vector and one functional axis [10], measuring two functional axes [11], aligning the sensor relative to one patient segment and by measuring a functional axis or a gravity vector [11] or by measuring anatomical axes using a dedicated calibration device [8]. However, there is a lack of justification about the choice to use an initialization method rather than another.

In this context, this study aims comparing the initialization methods regarding the error on the measurement of upper limb kinematics taking into account non-idealities in the respect of initialization procedures. The introduction of skin movement artefacts could introduce unnecessary noise in the evaluation of different initialization procedures and for this reason, they are not discussed in this study. This paper is organized as follows. Section II presents the model used for the upper limb and the number and position of sensors on the body. Section III provides a description of the implemented initialization procedures. Section IV describes how upper limb kinematics are calculated and the Section V presents the experimental setup and experimental methodology including the calculation of kinematics errors. Finally, the Section. VI shows and discusses the results obtained with both initialization procedures.

II. Upper limb model and sensors positioning

The kinematics must be measured in the bone frames while the sensors measure orientation in the Earth frame. It is therefore necessary to define an upper limb model in order to project measures in the skeleton frame.

A. Representation

The representation of an orientation is based on a quaternion q which has the advantage to describe any rotation in the most compact manner and without singularities comparing to other classical representations [17]. This representation is actually a representation of an Euler rotation, i.e. a rotation of an angle θ around a vector r_x, r_y, r_z expressed in the initial frame. The equivalent quaternion is then built by:

$$q = [\cos(\frac{\theta}{2}) \;\; r_x \sin(\frac{\theta}{2}) \;\; r_y \sin(\frac{\theta}{2}) \;\; r_z \sin(\frac{\theta}{2})]. \tag{1}$$

This work was supported by the FRIA (Fonds pour la Recherche dans l'Industrie et l'Agriculture).

D. Galinski and B. Dehez are with the Center for Research in Mechatronics, Université catholique de Louvain, Louvain-la-Neuve, 1348, Belgium. e-mail: daniel.galinski, bruno.dehez@uclouvain.be.

B. Upper limb model

The International Society of Biomechanics (ISB) has described all links of a real arm where each link can be represented by three angles [12]. Such a model is very complex and is unnecessarily complicated for our application. Several papers dealt with the simplification of a human arm model in order to obtain a model able to describe precisely enough the upper limb kinematics. Most of the consulted ones conclude that a model composed of seven revolute joints without translation parts is sufficient enough to describe this kinematics [13]–[15]. All of these models differ only by the Euler angles chosen for the shoulder representation. According to the reference axis defined in Fig. 1, this articular complex can be represented by a X-Z-Y [13], a Y-Z-Y [14] or a X-Y-Z suite [16]. However, to ensure consistency with the recommendations of ISB, we opted for a Y-X-Y representation for the shoulder complex illustrated on the Fig. 1.

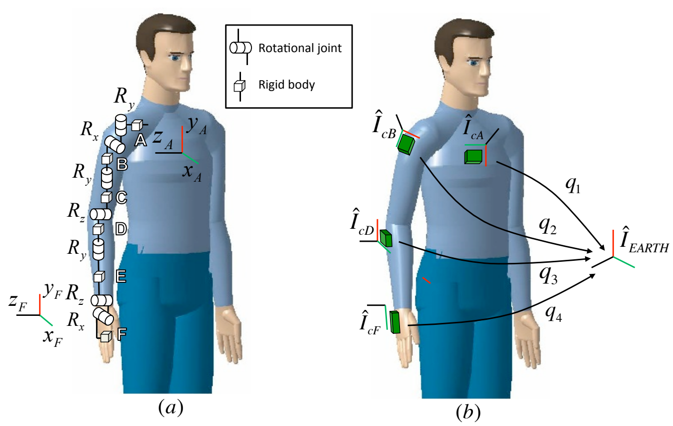

Fig. 1. (a) Model for the representation of the human upper limb. (b) The four sensors are placed on rigid bodies A-B-D-F and measure q_1, q_2, q_3 and q_4, the orientation of the Earth frame in their own frame.

C. Sensor placement

Inertial sensors could be mainly fixed on six different areas on a real arm. Neglecting the skin movement, these areas can be considered as rigidly linked to the skeleton chain of the arm corresponding to rigid bodies A, B, C, D, E, F as illustrated in Fig. 1. The sensor placement can be decided in order to minimize their number. As each sensor measures only its orientation relative to the Earth frame and if we assume that a sensor placed on a rigid body does not move during the acquisition period, two sensors can be separated from each other at most by three revolute joints in the model. Since our model has seven revolute joints at least, four inertial sensors have to be placed on the upper limb. The first one is placed on the trunk in order to act as a reference making the measures independent of the Earth frame. The three others can be placed on the upper limb following four configurations: A-B-D-F, A-C-E-F, A-C-D-F and A-B-E-F. The configuration selection can be guided by the necessity of avoiding singularities during the inverse kinematics calculation. Indeed, when three angles between two sensors are computed, a singularity, also called a gimbal lock, arises from the indistinguishability of changes in the first and third angle when the second angle is at some critical value [17]. Due to the large workspace of the shoulder, it is not possible to have an angle representation avoiding gimbal locks if the two first sensors are fixed to bodies A and C. Therefore, they must be placed on bodies A and B in order to have only two angles between them. The third sensor can be placed on bodies D or E. If it is placed on the body E, a gimbal lock is produced when the arm is along the trunk. It should then be placed on body D. The last sensor can be thus fixed on the hand, the body F, without any gimbal lock encountered in the workspace.

III. Initialization procedures

As the sensors are disposed on the upper limb with an unknown orientation relative to the model, the initialization procedure aims to determine the initial sensors orientation relative to the segment coordinate frame. This may be done by measuring two axes of bone segment frames in the sensor coordinate frames, the third one being deduced by vectorial product. These axes can be obtained by measuring two functional axes [11], by aligning one sensor relative to one patient segment and by measuring a functional axis or a gravity vector [11], or by measuring the gravity vector and one functional axis [10]. In another way, these axes can be obtained using dedicated calibration device [8]. In this paper, the two first techniques are implemented, i.e. without any additional calibration device, in order to find the quaternions equivalent to the orientation of each sensor relative to the patient segment, i.e. q_A, q_B, q_D and q_F illustrated on Fig. 2. Once these orientations are found, they are assumed to remain unchanged during the acquisition session.

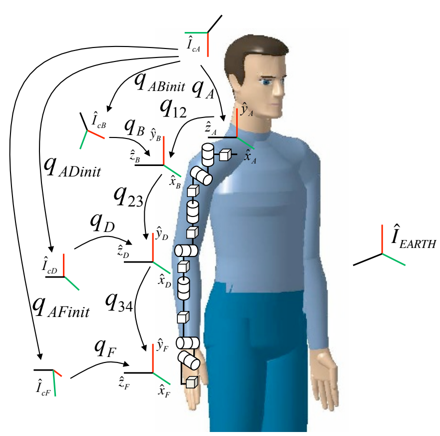

Fig. 2. Definition of the different quaternions used for initialization and kinematics calculation.

A. Init 1: Two functional axes using angular velocities

In this procedure all sensors are placed with a random orientation on the rigid bodies. In a first step, two single DOF movements are performed in order to deduce two functional axes. These are calculated from angular velocities measured by gyroscopes, as suggested Stokdijk et al. [18]. The first is a continuous abduction-adduction movement and it is performed for several seconds. If ω_B represents the angular velocity measured by sensor node B, $\hat{x}_B$ is obtained from averaged and normalized angular velocities data, then $\hat{x}_B = \omega_B / \|\omega_B\|$. In order to maximize the signal-to-noise ratio, a threshold of the maximum measured angular velocity is applied (30 % as presented in [7]). The second is a continuous antepulsion-retropulsion movement and it is performed during several seconds. As for the first movement, $\hat{z}_B = \omega_B / \|\omega_B\|$. The equivalent rotation matrix is finally obtained by $R_B = [\hat{x}_B^T \ \hat{y}_B^T \ \hat{z}_B^T]$ and the equivalent quaternion q_B is obtained by trigonometry, as explained in [17]. The second step aims to obtain the orientation of the three others sensors. For this step, the patient is placed in a reference position where the quaternions q_{12}, q_{23} and q_{34} are supposedly known. In our case, this reference corresponds to the arm positioned along the trunk. The quaternions q_{12}, q_{23} and q_{34} are therefore equal to identity and the orientations of the others sensors relative to their own frame given by:

$$\begin{aligned} q_A &= q_B \otimes q_{ABinit} \\ q_D &= q_A \otimes q_{ADinit}^* \\ q_F &= q_A \otimes q_{AFinit}^* \end{aligned} \tag{2}$$

where q_{AB}, q_{AD} and q_{AF} are the measurement of orientation of sensors B, D, F relative to the sensor A and where q^* represents the inverse of quaternion q.

B. Init 2: Vector gravity at first node

In this procedure the first sensor is positioned over the flat area of the sternum so as to ensure that the vector z_{cA} is aligned with the axis $\hat{z}_A$. While the others sensors are fixed on the arm with a random orientation. The first orientation axis of the first sensor node is thus imposed. The second requires in this first step of initialization that the patient is standing or sitting with the trunk aligned with the gravity vector. In this manner, the axis $\hat{y}_A$ is directly obtained by measuring the gravity vector using accelerometers of first sensor during a static trial of several seconds. The third axis $\hat{x}_A$ is produced by the cross product $\hat{y}_A \times \hat{z}_A$. The equivalent rotation matrix between the sensor A and the associated rigid body, i.e. the trunk, is given by $R_A = [\hat{x}_A^T \ \hat{y}_A^T \ \hat{z}_A^T]$ and the equivalent quaternion q_A is obtained by trigonometry. The second step is exactly the same as the one of the Init 1, but for obtaining q_B, q_D and q_F through:

$$\begin{aligned} q_B &= q_A \otimes q_{ABinit}^* \\ q_D &= q_A \otimes q_{ADinit}^* \\ q_F &= q_A \otimes q_{AFinit}^* \end{aligned} \tag{3}$$

IV. Kinematics

The initialization procedures aim to deduce the orientation of each sensor relative to the patient segments to which they are attached. If we suppose these relative orientation kept during the movements, the orientation of a segment relative to the previous one in its frame can therefore be found by:

$$\begin{aligned} q_{12} &= q_B \otimes q_2^* \otimes q_1 \otimes q_A^* \\ q_{23} &= q_D \otimes q_3^* \otimes q_2 \otimes q_B^* \\ q_{34} &= q_F \otimes q_4^* \otimes q_3 \otimes q_D^* \end{aligned} \tag{4}$$

Different kinematics data can be computed from these relative orientations and particularly the upper limb angles and the hand position.

A. Upper limb angles

The Euler angles are calculated by inverse kinematics from the measured relative quaternions in the segment space. All seven angles can be calculated [17]:

1) Shoulder : antepulsion-retropulsion ϕ_1 and abduction-adduction ϕ_2:

$$\begin{aligned} \phi_1 &= \text{atan2}(-2q_{12}(2)q_{12}(4) - 2q_{12}(1)q_{12}(3), \\ &\qquad q_{12}^2(1) + q_{12}^2(2) - q_{12}^2(3) - q_{12}^2(4)) \\ \phi_2 &= \text{atan2}(-2q_{12}(3)q_{12}(4) + 2q_{12}(1)q_{12}(2), \\ &\qquad q_{12}^2(1) - q_{12}^2(2) + q_{12}^2(3) - q_{12}^2(4)) \end{aligned}$$

2) Arm : humeral internal-external rotation ϕ_3 and elbow flexion-extension ϕ_4:

$$\begin{aligned} \phi_3 &= \text{atan2}(2q_{23}(2)q_{23}(4) + 2q_{23}(1)q_{23}(3), \\ &\qquad q_{23}^2(1) - q_{23}^2(2) - q_{23}^2(3) + q_{23}^2(4)) \\ \phi_4 &= \text{atan2}(2q_{23}(2)q_{23}(3) + 2q_{23}(1)q_{23}(4), \\ &\qquad q_{23}^2(1) - q_{23}^2(2) + q_{23}^2(3) - q_{23}^2(4)) \end{aligned}$$

3) Forearm : pronation-supination ϕ_5, wrist abduction-adduction ϕ_6 and wrist flexion-extension ϕ_7:

$$\begin{aligned} \phi_5 &= \text{atan2}(-2q_{34}(3)q_{34}(4) - 2q_{34}(1)q_{34}(2), \\ &\qquad q_{34}^2(1) - q_{34}^2(2) + q_{34}^2(3) - q_{34}^2(4)) \\ \phi_6 &= \text{asin}\,(2q_{34}(2)q_{34}(3) + 2q_{34}(1)q_{34}(4)) \\ \phi_7 &= \text{atan2}(-2q_{34}(2)q_{34}(4) + 2q_{34}(1)q_{34}(3), \\ &\qquad q_{34}^2(1) + q_{34}^2(2) - q_{34}^2(3) - q_{34}^2(4)) \end{aligned}$$

B. Hand position

The cartesian position of the hand's center of mass relative to the glenohumeral joint in the trunk frame can be calculated from:

$$XYZ = \sum_{i=1}^{3} v_i^{rot} \tag{5}$$

where v_i^{rot} are the expression in the segment frame of v_i, the vectors of norm equal to the limb lengths aligned with limb segments. These are linked through the relations:

$$\begin{aligned} v_1^{rot} &= q_{12}^* \otimes v_1 \otimes q_{12} \\ v_2^{rot} &= (q_{23} \otimes q_{12})^* \otimes v_2 \otimes (q_{23} \otimes q_{12}) \\ v_3^{rot} &= (q_{34} \otimes q_{23} \otimes q_{12})^* \otimes v_3 \otimes (q_{34} \otimes q_{23} \otimes q_{12}) \end{aligned} \tag{6}$$

V. Experiments

This section gives some details about the hardware and the software implementation of the instrumentation. It also presents the test bench, the method and the performance criteria used to evaluate the initialization procedures.

A. Hardware and software implementation

We opted for MARG sensors from the X-io company (UK, Bristol). These sensors were packaged with a battery and can be fixed on the arm using Hook-and-loop fasteners. One packaged MARG sensor weighs 42 [g] and has size of 69x43x17 [mm^3] (Fig. 3). The sensors are filtered and calibrated on-board and the filtered orientation is sent in a quaternion representation to a computer via Bluetooth.

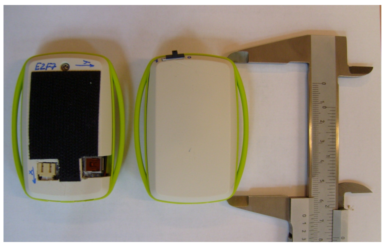

Fig. 3. Package containing a x-IMU MARG sensor and a battery. One side is equipped with Velcro for fixing.

The initialization procedures, the measurements, the kinematics calculations and the graphic interfaces are implemented in real-time in C#, using the C# source code and API's provided by the X-io company. The receiving computer is equipped with a master Bluetooth modem and all communication data flows through four emulated COM ports.

B. Test bench

The evaluation of the instrumentation and the initializations procedures were performed on an artificial arm rather than on a real one in order to evaluate the proper functioning of the algorithms without taking into account or discussing about the impact of skin artefacts on the initialization procedure or the inaccuracy of the arm model used. An artificial anthropomorphic arm has been designed and prototyped (Fig. 4). Its structure is exactly the same as the model presented in Fig. 1. The segments are made from aluminium and are long as the human mean segment lengths found in [19]. Segments are linked together by friction hinges equipped with absolute encoders of 4096 pulses per revolution which define the reference of angular position.

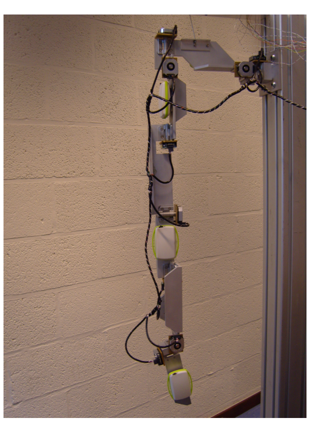

Fig. 4. The artificial anthropomorphic upper limb equipped with absolute encoders.

C. Method

Five trials were performed. For each trial, the MARG sensors were first placed with a random orientation on the upper limb as specified in Sect. II-C. Next, four different initialization procedures were performed:

1) "Ideal Init 1" as exposed in Sect. III-A: the initialization procedure was respected as best as possible.
2) "Non-ideal Init 1": the two initialization movements were performed with a $10°$ coupling with an another axis and the upper limb was positioned with an abduction of $10°$ during the recording of the reference position.
3) "Ideal Init 2" as exposed in Sect. III-B: the initialization procedure was respected as best as possible.
4) "Non-ideal Init 2": the upper limb was positioned with an abduction of $10°$ during the initialization procedure and recording of the reference position.

When the four initialization procedures were done, four Activities of Daily Living (ADL) movements were performed in order to evaluate the performance of the kinematics tracking in real conditions:

1) Reach a glass above the transversal plane of shoulder and drink it several times.
2) Do perineal care several times.
3) Comb hair several times.
4) Achieve a triple extension position from a triple flexion position (shoulder, elbow and wrist maximally flexed).

These ADL movements were selected from [20] and [21] for their diversity and their complementarity regarding the workspace exploration. These were executed manually on the artificial arm for each new trial.

D. Performance criteria

The quality and the robustness of the initialization procedures on the upper limb joint angles and on the hand position estimations are evaluated through two criteria. The first is the root mean squared error (RMSE) of the joint angles deduced from the MARG sensors measurement and the angles measured by the coders:

$$RMSE_i = \sqrt{\frac{1}{T}\sum_{k=1}^{T}(\phi_i^M(k) - \phi_i^C(k))^2} \quad (7)$$

where the subscript i refers to the joint, the superscripts M and C refer to the measures obtained from the MARG sensors and from the coders respectively and the variable k is the sample number. The second criteria is the RMSE of the distance ΔXYZ between the distal position calculated from MARG sensors measurements and the distal position calculated using coders represents the distal position error. The distal position measured by MARG sensors is computed by using Eq. 5 and the averaged human male segment lengths presented in [19]: arm is 28.2 [cm] long, forearm is 26.9 [cm] long and hand is 8.6 [cm] long. The RMSE of this distal position is then directly calculated by:

$$RMSE_{XYZ} = \sqrt{\frac{1}{T}\sum_{k=1}^{T}\Delta XYZ(k)^2} \quad (8)$$

VI. Results and discussion

Fig. 5 shows the estimations of the joint angles and of the norm of the error on the hand position for the 'reach and drink' movement according to the four initialization procedures. These results show a strong correlation between the joint angles measured by the MARG sensors and the coders. However, they also reveal deviations for both initialization procedures, even with the ideals. The most important are observed on the internal/external rotation of the shoulder and the pronation/supination of the forearm. These deviations can be attributed to the accuracy and the precision of the sensor of course, but they also highlight that the initializations can not be perfectly executed even in the best conditions. Relative to the ideal Init 1, ideal Init 2 shows more important deviations. This lead us to believe that this initialization is intrinsically more difficult to perform properly or is more sensitive to the strict observance of its procedure. Finally, it can be observed on Fig. 5 that the Init 1 remains better than Init 2 even when the initialization procedures entail obvious non-idealities.

These observations are confirmed by the Fig. 6 that provides a statistic analysis of the performance criteria on twenty ADL movements, i.e. five trials of four ADL. In this figure, the median values are illustrated by a $\odot$, the inter-quantile ranges are represented by the upper and lower limits of the broad line, the full ranges are represented by the upper and lower limits of narrow lines and the outliers are illustrated by a $\circ$. In accordance with Fig. 5, the Init 1 is more accurate than Init 2 for the computation of the hand position ($p < 0.001$) and of the joint angles, except for pronation/supination. Performing an Init 1, the RMSE on the hand position does not exceed 4.36 [cm] while it reaches 8.70 [cm] for Init 2. On the other hand, Fig. 6 shows that the two initialization procedures have almost the same sensivity to non-idealities.

In addition to these observations, it is important to underline that the Init 1 procedure requires two movements and does not require any aligning of trunk or upper limb with gravity which can be an additional source of error during Init 2.

VII. Conclusion

In this study, two initialization procedures has been described and compared for upper limb kinematics estimations using MARG sensors. Their robustness regarding the non perfect execution of the procedures was also discussed. Skin movement artefacts inherent in any human kinematics estimation was not included because they affect the different calibration methods in the same way. Their inclusion would therefore complicate unnecessarily the discussion about the choice of an initialization procedure rather than another.

The results have shown that an initialization made through functional axes is less dependent to the strict observance of the initialization procedure. However, initialization made through alignment on gravity vector could make sense for weak patients because it does not requires any movements which can be a source of error if they are not correctly executed by weak patients. Given that and the analysis presented, it seems clear that an initialization made through functional axes is the recommended procedure if functional movements can be done by the patient.

References

[1] Y. Bejot, I. Benatru, O. Rouaud, A. Fromont, J. P. Besancenot, T. Moreau, and M. Giroud, "Epidemiology of stroke in europe: Geographic and environmental differences," *Journal of the Neurological Sciences*, vol. 262, no. 12, pp. 85 – 88, 2007.

[2] R. Colombo, F. Pisano, S. Micera, A. Mazzone, C. Delconte, M. Carrozza, P. Dario, and G. Minuco, "Robotic techniques for upper limb evaluation and rehabilitation of stroke patients," *Neural Systems and Rehabilitation Engineering, IEEE Transactions on*, vol. 13, no. 3, pp. 311–324, 2005.

[3] A. Mirelman, P. Bonato, and J. Deutsch, "Effects of training with a robot-virtual reality system compared with a robot alone on the gait of individuals after stroke," *Stroke*, vol. 40, no. 1, pp. 169–174, 2009.

[4] V. S. Ramachandran and E. L. Altschuler, "The use of visual feedback, in particular mirror visual feedback, in restoring brain function," *Brain*, vol. 132, no. 7, pp. 1693–1710, 2009.

[5] H. Wu, J. Liu, H. Handroos, B. Miraftabi, A. Heinonen, S. Peurala, I. Tarkka, M. Rossi, and S. Nousiainen, "Virtual reality based robotic therapy for stroke rehabilitation: An initial study," in *2011 IEEE International Conference on Mechatronics and Automation, ICMA 2011*, 2011, pp. 1196–1200.

[6] H. Zhou and H. Hu, "Human motion tracking for rehabilitation–A survey," *Biomedical Signal Processing and Control*, vol. 3, no. 1, pp. 1–18, 2008.

[7] W. De Vries, H. Veeger, A. Cutti, C. Baten, and F. Van der Helm, "Functionally interpretable local coordinate systems for the upper extremity using inertial & magnetic measurement systems," *Journal of biomechanics*, vol. 43, no. 10, pp. 1983–1988, 2010.

[8] P. Picerno, A. Cereatti, and A. Cappozzo, "Joint kinematics estimate using wearable inertial and magnetic sensing modules," *Gait & posture*, vol. 28, no. 4, pp. 588–595, 2008.

[9] V. van Acht, E. Bongers, N. Lambert, and R. Verberne, "Miniature wireless inertial sensor for measuring human motions," in *Engineering in Medicine and Biology Society, 2007. EMBS 2007. 29th Annual International Conference of the IEEE*. IEEE, 2007, pp. 6278–6281.

[10] H. Luinge, P. Veltink, and C. Baten, "Ambulatory measurement of arm orientation," *Journal of Biomechanics*, vol. 40, no. 1, pp. 78–85, 2007.

[11] A. Cutti, A. Giovanardi, L. Rocchi, A. Davalli, and R. Sacchetti, "Ambulatory measurement of shoulder and elbow kinematics through inertial and magnetic sensors," *Medical and Biological Engineering and Computing*, vol. 46, no. 2, pp. 169–178, 2008.

[12] G. Wu, F. Van der Helm, H. Veeger, M. Makhsous, P. Van Roy, C. Anglin, J. Nagels, A. Karduna, and K. McQuade, "ISB recommendation on definitions of joint coordinate systems of various joints for the reporting of human joint motion–Part II: shoulder, elbow, wrist and hand," *Journal of biomechanics*, vol. 38, no. 5, pp. 981–992, 2005.

[13] N. Klopčar and J. Lenarčič, "Kinematic model for determination of human arm reachable workspace," *Meccanica*, vol. 40, no. 2, pp. 203–219, 2005.

[14] A. Kontaxis, A. Cutti, G. Johnson, and H. Veeger, "A framework for the definition of standardized protocols for measuring upper-extremity kinematics." *Clinical biomechanics (Bristol, Avon)*, vol. 24, no. 3, p. 246, 2009.

[15] R. Prokopenko, A. Frolov, E. Biryukova, and A. Roby-Brami, "Assessment of the accuracy of a human arm model with seven degrees of freedom," *Journal of biomechanics*, vol. 34, no. 2, pp. 177–185, 2001.

[16] J. Lenarcic and M. Stanisic, "A humanoid shoulder complex and the humeral pointing kinematics," *Robotics and Automation, IEEE Transactions on*, vol. 19, no. 3, pp. 499–506, 2003.

[17] J. Diebel, "Representing attitude: Euler angles, unit quaternions, and rotation vectors," *Matrix*, 2006.

[18] M. Stokdijk, M. Biegstraaten, W. Ormel, Y. de Boer, H. Veeger, and P. Rozing, "Determining the optimal flexion-extension axis of the elbow in vivo–a study of interobserver and intraobserver reliability," *Journal of Biomechanics*, vol. 33, no. 9, pp. 1139–1145, 2000.

[19] P. De Leva, "Adjustments to zatsiorsky-seluyanov's segment inertia parameters," *Journal of biomechanics*, vol. 29, no. 9, pp. 1223–1230, 1996.

[20] C. van Andel, N. Wolterbeek, C. Doorenbosch, D. Veeger, and J. Harlaar, "Complete 3d kinematics of upper extremity functional tasks," *Gait & posture*, vol. 27, no. 1, pp. 120–127, 2008.

[21] D. Magermans, E. Chadwick, H. Veeger, and F. Van Der Helm, "Requirements for upper extremity motions during activities of daily living," *Clinical Biomechanics*, vol. 20, no. 6, pp. 591–599, 2005.

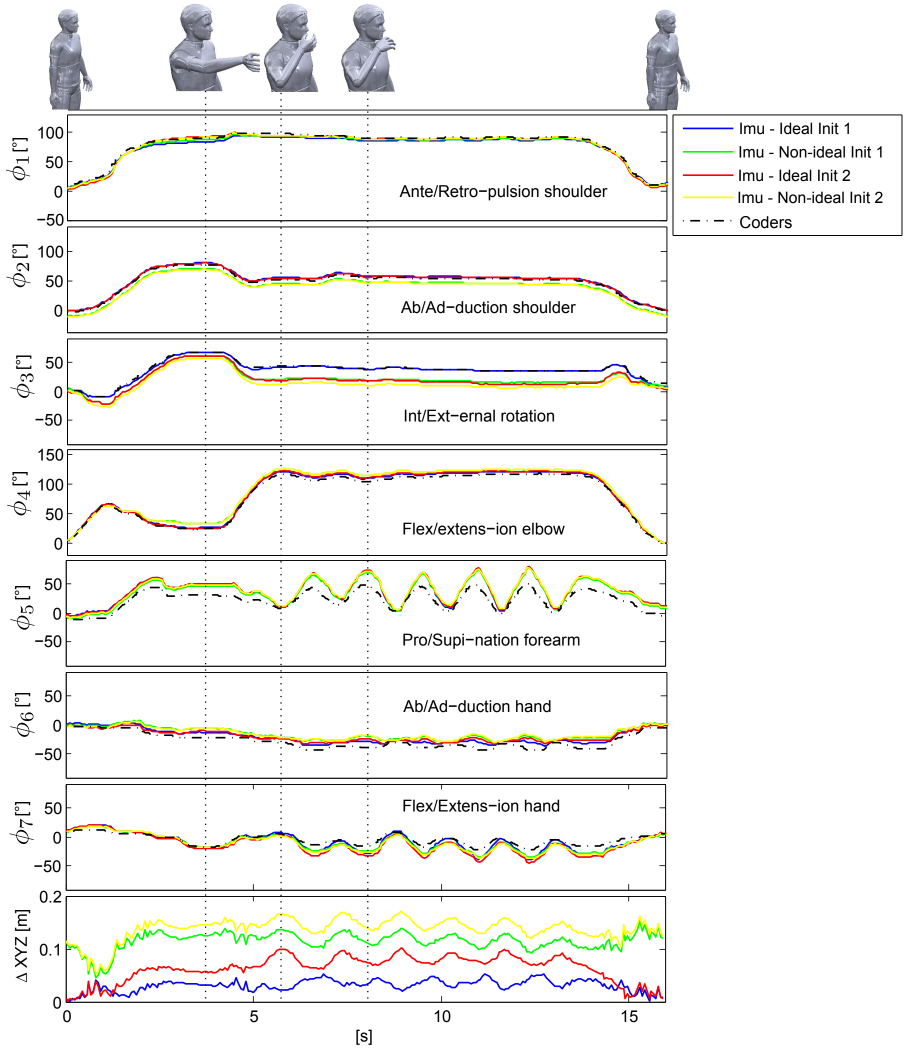

Fig. 5. Upper limb joint angles measurements for a reach and drink ADL.

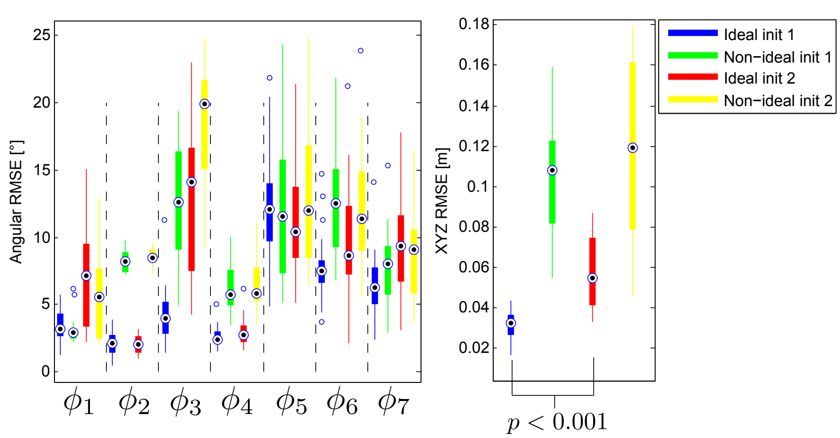

Fig. 6. Box plot of the RMSEs of measuring upper limb kinematics (joint angles and distal position).